

Kinetics and Thermochemistry of the $\text{Cl}(^2\text{P}_j) + \text{C}_2\text{Cl}_4$ Association Reaction

J. M. Nicovich and S. Wang[†]

Georgia Tech Research Institute, Georgia Institute of Technology, Atlanta, Georgia 30332

M. L. McKee

Department of Chemistry, Auburn University, Auburn, Alabama 36849

P. H. Wine*

School of Chemistry and Biochemistry, School of Earth and Atmospheric Sciences,
and Georgia Tech Research Institute, Georgia Institute of Technology, Atlanta, Georgia 30332

Received: August 15, 1995; In Final Form: October 12, 1995[⊗]

A laser flash photolysis–resonance fluorescence technique has been employed to study the kinetics of the $\text{Cl}(^2\text{P}_j) + \text{C}_2\text{Cl}_4$ association reaction as a function of temperature (231–390 K) and pressure (3–700 Torr) in nitrogen buffer gas. The reaction is found to be in the falloff regime between third and second order over the range of conditions investigated, although the second-order limit is approached at the highest pressures and lowest temperatures. At temperatures below 300 K, the association reaction is found to be irreversible on the experimental time scale of ~ 20 ms. The kinetic data at $T < 300$ K have been employed to obtain falloff parameters in a convenient format for atmospheric modeling. At temperatures above 330 K, reversible addition is observed, thus allowing equilibrium constants for C_2Cl_5 formation and dissociation to be determined. Second- and third-law analyses of the equilibrium data lead to the following thermochemical parameters for the association reaction: $\Delta H^\circ_{298} = -18.1 \pm 1.3$ kcal mol⁻¹, $\Delta H^\circ_0 = -17.6 \pm 1.3$ kcal mol⁻¹, and $\Delta S^\circ_{298} = -27.7 \pm 3.0$ cal mol⁻¹ K⁻¹. In conjunction with the well-known heats of formation of $\text{Cl}(^2\text{P}_j)$ and C_2Cl_4 , the above ΔH values lead to the following heats of formation for C_2Cl_5 at 298 and 0 K: $\Delta H^\circ_{f,298} = 8.0 \pm 1.3$ kcal mol⁻¹ and $\Delta H^\circ_{f,0} = 8.1 \pm 1.5$ kcal mol⁻¹. The kinetic and thermochemical parameters reported above are compared with other reported values, and the significance of reported association rate coefficients for understanding tropospheric chlorine chemistry is discussed.

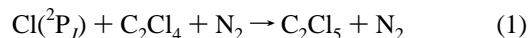
Introduction

Tetrachloroethylene (C_2Cl_4) is used widely for dry cleaning, for metal degreasing, and as an industrial solvent.^{1,2} Global production of C_2Cl_4 over the decade from the early 1980s to the early 1990s averaged around 600 ktons yr⁻¹, and a majority of this production has found its way into the atmosphere.¹ Field observations of the global distribution of atmospheric C_2Cl_4 have been employed in conjunction with spatially resolved emissions data to deduce an average tropospheric lifetime of about 0.4 yr.^{1,3,4} This lifetime is consistent with the notion that C_2Cl_4 removal from the troposphere is dominated by reaction with the OH radical, although uncertainties in the OH + C_2Cl_4 rate coefficient and in tropospheric OH concentrations are such that the lifetime for C_2Cl_4 toward reaction with OH could be anywhere in the range 0.20–0.65 yr.²

Comparison of available kinetic data for the OH + C_2Cl_4 reaction^{5–8} with available data for the $\text{Cl}(^2\text{P}_j) + \text{C}_2\text{Cl}_4$ reaction^{9–16} suggests that the $\text{Cl}(^2\text{P}_j) + \text{C}_2\text{Cl}_4$ rate coefficient is several hundred times faster than the OH + C_2Cl_4 rate coefficient at tropospheric temperatures and pressures. Until recently, it has been thought that chlorine atom levels in the troposphere were so low that $\text{Cl}(^2\text{P}_j)$ could not be an important tropospheric reactant. However, evidence is now mounting which suggests that chlorine atom levels in the marine boundary layer may be as much as one-tenth as high as OH levels,^{17,18} with the chlorine

atom source probably being photochemically labile chlorine species such as Cl_2 and ClNO_2 produced via heterogeneous reactions on the surfaces of moist sea salt particles.¹⁹ Hence, it appears that in certain regions of the troposphere reaction with $\text{Cl}(^2\text{P}_j)$ is an important removal mechanism for C_2Cl_4 .

Reaction 1 must proceed via an addition mechanism, i.e., for N_2 buffer gas,



The current state of knowledge concerning the atmospheric oxidation mechanism for C_2Cl_5 has recently been reviewed by Franklin.² Phosgene (Cl_2CO) is the major end product, but significant yields of carbon tetrachloride, a compound with a large ozone depletion potential, have been reported.²⁰ While CCl_4 can be produced via the gas phase photolysis of the intermediate photooxidation product CCl_3CClO , it is now thought that most CCl_4 observed in laboratory photooxidation studies is formed by heterogeneous photochemical processes.² Hence, yields of CCl_4 observed in laboratory “smog chamber” studies may be larger than those which would actually be produced in the atmosphere.

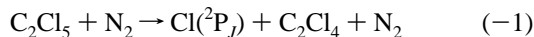
While numerous kinetics studies of reaction 1 have been reported,^{9–16} the temperature and pressure dependences of the rate coefficient have not been systematically investigated. In this paper we report the results of experiments where laser flash photolysis of $\text{Cl}_2/\text{C}_2\text{Cl}_4/\text{N}_2$ mixtures has been coupled with $\text{Cl}(^2\text{P}_j)$ detection by time-resolved atomic resonance fluorescence spectroscopy to investigate the kinetics of reaction 1 over the temperature range 231–298 K and the pressure range 3–700

[†] Present address: Dalian Institute of Chemical Physics, Chinese Academy of Sciences, P.O. Box 110, Dalian, People's Republic of China.

* To whom correspondence should be addressed.

[⊗] Abstract published in *Advance ACS Abstracts*, December 15, 1995.

Torr; over this range of experimental conditions the reaction is found to be in the falloff regime between third and second order, although the high-pressure second-order limit is approached at the low-temperature and high-pressure limits of the range of conditions investigated. We also report experiments at higher temperatures (332–390 K) where Cl(²P_J) regeneration is observed on the experimental time scale (10⁻⁵–10⁻² s), thus indicating the occurrence of the reverse dissociation reaction:



Analysis of equilibration kinetics as a function of temperature provides information about the thermochemistry of reaction 1.

Experimental Technique

The laser flash photolysis–resonance fluorescence apparatus employed in this study was similar to those employed in our laboratory in several previous studies of chlorine atom kinetics.^{21,22} Important features of the apparatus and experimental techniques which are specific to this study are described below.

Chlorine atoms were produced by 355 nm laser flash photolysis of Cl₂. Third harmonic radiation from a Quanta Ray Model DCR-2 Nd:YAG laser provided the photolytic light source. The photolysis laser could deliver up to 1 × 10¹⁷ photons per pulse at a repetition rate of up to 10 Hz; the pulse width was 6 ns. Fluences employed in this study ranged from 5 to 50 mJ cm⁻² pulse⁻¹.

In order to avoid accumulation of photochemically generated reactive species, all experiments were carried out under “slow flow” conditions. The linear flow rate through the reactor was typically 3 cm s⁻¹ while the laser repetition rate was varied over the range 2–10 Hz. (It was 2 Hz in most experiments at *T* < 300 K and 10 Hz in most experiments at *T* > 330 K.) Since the direction of flow was perpendicular to the photolysis laser beam, no volume element of the reaction mixture was subjected to more than a few laser shots. Molecular chlorine (Cl₂) and C₂Cl₄ were flowed into the reaction cell from 12 L Pyrex bulbs containing dilute mixtures in nitrogen buffer gas, while N₂ flowed directly from its high-pressure storage tank. The Cl₂/N₂ mixture, C₂Cl₄/N₂ mixture, and additional N₂ were premixed before entering the reaction cell. Concentrations of each component in the reaction mixture were determined from measurements of the appropriate mass flow rates and the total pressure. The C₂Cl₄ concentration was also measured *in situ* in the slow flow system by UV photometry at 228.8 nm using a cadmium penray lamp as the light source. The C₂Cl₄ absorption cross section at 228.8 nm was measured during the course of this study and was found to be 8.36 × 10⁻¹⁸ cm². Kinetics results were found to be independent of whether the 60.3–201 cm long absorption cell was positioned upstream or downstream from the reaction cell. In the lowest pressure experiments a small correction was required for the pressure differential between the absorption cell and the reaction cell; the pressure differential never exceeded 1%. In all photometric measurements (including the absorption cross section measurements) the absorption cell temperature was 297 ± 2 K.

The gases used in this study had the following stated minimum purities: N₂, 99.999%; Cl₂, 99.9%.²³ Nitrogen was used as supplied while Cl₂ was degassed at 77 K before being used to prepare mixtures with N₂. The liquid C₂Cl₄ sample had a stated purity of 99+%. It was transferred under nitrogen atmosphere into a vial fitted with a high vacuum stopcock and then degassed repeatedly at 77 K before being used to prepare mixtures with N₂.

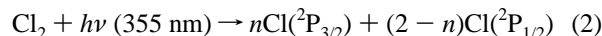
TABLE 1: Summary of Kinetic Data for the Reaction Cl(²P_J) + C₂Cl₄ + N₂ → C₂Cl₅ + N₂ Obtained under Experimental Conditions (*T* < 300 K) Where the Reaction Was Irreversible on the Time Scale for Cl(²P_J) Decay^a

<i>T</i>	<i>P</i>	[Cl ₂]	[Cl] _{<i>t</i>=0}	[C ₂ Cl ₄] _{max}	no. of expts ^b	<i>k</i> ' _{max}	<i>k</i> ₁ ± 2σ ^c
231	3.1	77	1.9	6000	6	17500	28.1 ± 0.8
	6.2	69	0.8	2750	5	9300	33.1 ± 1.1
	26	63	0.6	2490	6	10700	43.0 ± 2.5
	101	60	0.6	2320	6	12200	50.3 ± 3.1
	401	61	0.6	1870	6	9770	51.6 ± 0.9
	702	99	1.4	2500	6	12200	48.0 ± 2.4
260	3.1	22–76	1.6	7330	9	11900	15.6 ± 0.3
	6.2	62	0.7	2330	6	5080	20.3 ± 1.8
	26	61	0.6	2130	6	7290	33.6 ± 1.2
	101	54	0.6	2070	5	8630	41.5 ± 3.2
	402	57	0.7	1630	5	7150	42.8 ± 3.1
	702	85	0.9	2070	5	9740	46.5 ± 2.3
297	3.1	70	1.9	6750	10	5700	7.9 ± 0.3
	6.1	27–240	0.2–1.5	2590	20	3020	11.1 ± 0.8
	13	10–56	0.1–0.7	2120	10	3140	14.4 ± 0.9
	26	10–79	0.1–1.8	3370	21	6490	18.7 ± 0.7
	26	43	0.8	3230	10	6150	18.6 ± 1.1 ^d
	52	35	0.6	1790	5	4110	22.6 ± 0.8
	101	54	0.9	1620	7	4370	26.9 ± 0.8
	201	32–93	0.3–1.0	2360	12	7830	32.5 ± 2.1
	401	64	1.3	1700	8	6560	37.8 ± 3.2
	701	10	1.3	1760	14	7600	38.7 ± 2.5

^a Units: *T* (K); *P* (Torr); concentrations (10¹¹ molecules cm⁻³); *k*'_{max} (s⁻¹); *k*₁ (10⁻¹² cm³ molecule⁻¹ s⁻¹). ^b Expt ≡ determination of one pseudo-first-order decay rate. ^c Errors represent precision only. ^d 1.0 × 10¹⁵ CF₂Cl₂ per cm³ added to reaction mixture.

Results and Discussion

In all experiments, chlorine atoms were generated by laser flash photolysis of Cl₂:



The fraction of chlorine atoms generated in the excited spin–orbit state, Cl(²P_{1/2}), is thought to be very small, i.e., less than 0.01.^{24,25} Recently, it has been reported that the rate coefficient for Cl(²P_{1/2}) quenching by N₂ is considerably slower than previously thought, i.e., 5.0 × 10⁻¹⁵ cm³ molecule⁻¹ s⁻¹.²⁶ However, on the basis of reported rate coefficients for Cl(²P_{1/2}) deactivation by saturated halocarbons (all gas kinetic except, possibly, CF₄),^{26–29} we expect that the rate coefficient for Cl(²P_{1/2}) deactivation by C₂Cl₄ is very fast, i.e., (2 ± 1) × 10⁻¹⁰ cm³ molecule⁻¹ s⁻¹. Hence, it seems safe to assume that all Cl(²P_J) + C₂Cl₄ kinetic data are representative of an equilibrium mixture of Cl(²P_{1/2}) and Cl(²P_{3/2}). As a further check on the assumption of spin state equilibration, the rate coefficient at *T* = 297 K and *P* = 26 Torr was measured with and without CF₂Cl₂, a very efficient Cl(²P_{1/2}) quencher,^{26,28,29} added to the reaction mixture; as expected, this variation in experimental conditions had no effect on the observed reaction rate (see Table 1). The equilibrium fraction of chlorine atoms in the ²P_{1/2} state ranges from 0.0021 at 231 K to 0.019 at 390 K. It is worth noting that, given the small fraction of chlorine atoms in the ²P_{1/2} state and the fast values for *k*₁ which are measured (Tables 1 and 2), it must be the case that observed reactivity is dominated by chlorine atoms in the ²P_{3/2} state.

All experiments were carried out under pseudo-first-order conditions with C₂Cl₄ in large excess over Cl(²P_J). Hence, in the absence of side reactions that remove or produce chlorine atoms, the Cl(²P_J) temporal profile following the laser flash would be described by the relationship

$$\ln\{[\text{Cl}(\text{}^2\text{P}_J)]_0/[\text{Cl}(\text{}^2\text{P}_J)]_t\} = (k_1[\text{C}_2\text{Cl}_4] + k_3)t = k't \quad (I)$$

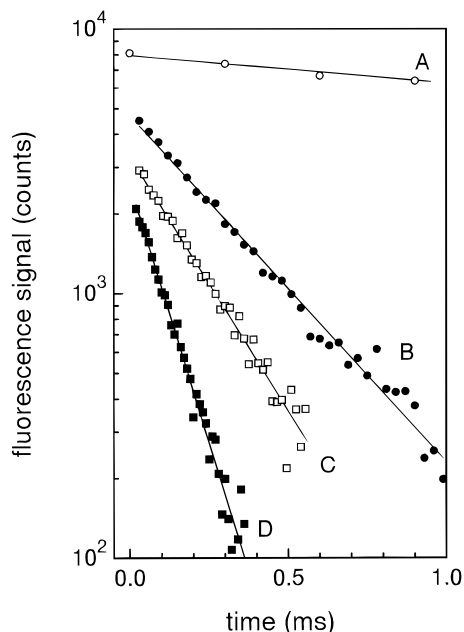


Figure 1. Typical $\text{Cl}(^2\text{P}_j)$ temporal profiles observed at $T < 300$ K. Experimental conditions: $T = 259$ K; $P = 100$ Torr; $M = \text{N}_2$; $[\text{Cl}_2] = 5.4 \times 10^{12}$ molecules cm^{-3} ; $[\text{Cl}]_0 = 5.6 \times 10^{10}$ atoms cm^{-3} ; $[\text{C}_2\text{Cl}_4]$ in units of 10^{14} molecules cm^{-3} (A) 0, (B) 0.724, (C) 1.07, and (D) 2.07; number of laser shots averaged (A) 400, (B) 2000, (C) 2000, and (D) 3000. Solid lines are obtained from least-squares analyses and give the following pseudo-first-order decay rates in units of s^{-1} : (A) 245, (B) 3250, (C) 4560, and (D) 8630. For the sake of clarity, traces A and D are scaled by factors of 0.9 and 1.5, respectively.

where k_3 is the rate coefficient for the process

$\text{Cl} \rightarrow$ first-order loss by diffusion from the detector field of view and/or reaction with background impurities (3)

The bimolecular rate coefficients of interest, $k_1([\text{N}_2], T)$, are determined from the slopes of k' versus $[\text{C}_2\text{Cl}_4]$ plots for data obtained at constant $[\text{N}_2]$ and T and under conditions where N_2 is the dominant third body collider with the energized C_2Cl_5 complex. Observation of $\text{Cl}(^2\text{P}_j)$ temporal profiles that are exponential, i.e., obey eq I, a linear dependence of k' on $[\text{C}_2\text{Cl}_4]$, and invariance of k' to variation in laser photon fluence and photolyte concentration strongly suggests that reactions 1 and 3 are, indeed, the only processes that significantly affect the $\text{Cl}(^2\text{P}_j)$ time history.

Kinetics at $T < 300$ K. For all experiments carried out at temperatures below 300 K, well-behaved pseudo-first-order kinetics were observed; i.e., $\text{Cl}(^2\text{P}_j)$ temporal profiles obeyed eq I, and k' increased linearly with increasing $[\text{C}_2\text{Cl}_4]$ but was independent of laser photon fluence and photolyte concentration. Typical data are shown in Figures 1–3. Measured bimolecular rate coefficients, $k_1([\text{N}_2], T)$ are summarized in Table 1. As expected for an association reaction in the non-high-pressure-limit regime, $k_1([\text{N}_2], T)$ is found to increase with increasing pressure and with decreasing temperature.

Parametrization of $k_1([\text{N}_2], T)$ for Atmospheric Modeling. For purposes of atmospheric modeling, it is convenient to generate a mathematical expression that can be used to compute $k_1([\text{N}_2], T)$ over the range of relevant temperatures and pressures. (The efficiency of O_2 as a third body collider is generally very similar to that of N_2 .) The expression generally used for this purpose is³⁰

$$k_1([\text{N}_2], T) = \{A/[1 + (A/B)]\}F_c^{\{1 + [\log(A/B)]^2\}^{-1}} \quad (\text{II})$$

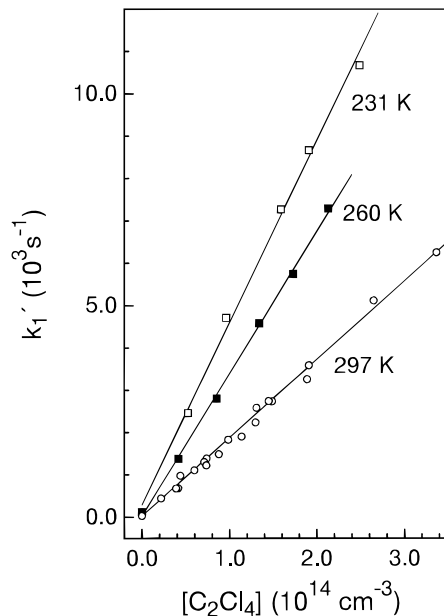


Figure 2. Plots of k' , the $\text{Cl}(^2\text{P}_j)$ pseudo-first-order decay rate, versus C_2Cl_4 concentration, as a function of temperature for data obtained at $P = 26$ Torr of N_2 with no added CF_2Cl_2 . The solid lines are obtained from linear least-squares analyses and the resulting rate coefficients, i.e., the slopes of the plots, are listed in Table 1.

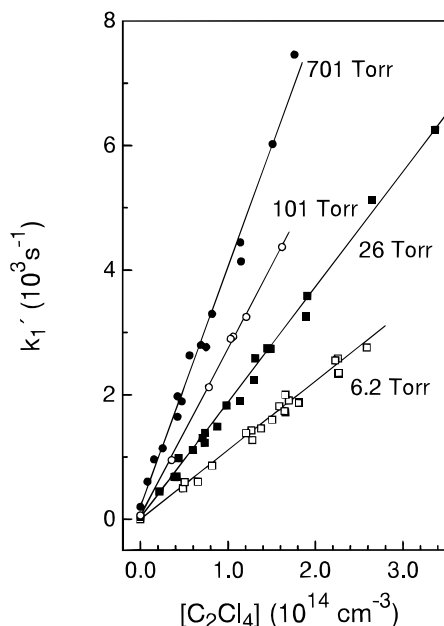


Figure 3. Plots of k' , the $\text{Cl}(^2\text{P}_j)$ pseudo-first-order decay rate, versus C_2Cl_4 concentration as a function of pressure for data obtained at $T = 297$ K. The solid lines are obtained from linear least-squares analyses, and the resulting rate coefficients, i.e., the slopes of the plots, are listed in Table 1.

where

$$A = k_{1,0}(T)[\text{N}_2] = k_{1,0}(300 \text{ K})(T/300)^{-n}[\text{N}_2] \quad (\text{III})$$

$$B = k_{1,\infty}(T) = k_{1,\infty}(300 \text{ K})(T/300)^{-m} \quad (\text{IV})$$

$$F_c = 0.6 \quad (\text{V})$$

In the above expression, $k_{1,0}$ and $k_{1,\infty}$ are approximations to the low- and high-pressure limit rate coefficients for reaction 1, and F_c is the “broadening parameter”. The value $F_c = 0.6$ is found to fit data for a wide variety of atmospheric reactions reasonably

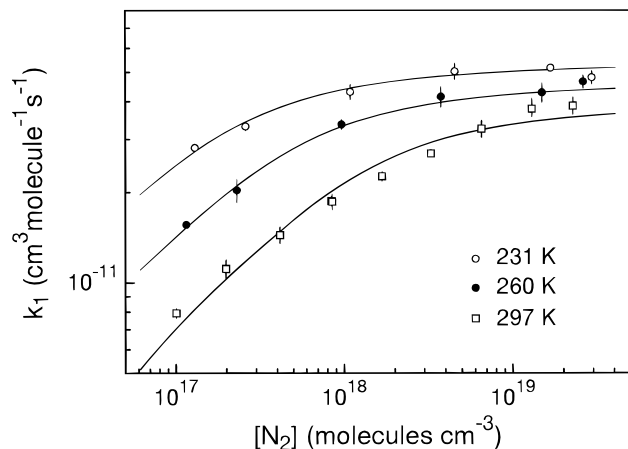


Figure 4. Falloff curves for the reaction $\text{Cl}({}^2\text{P}_J) + \text{C}_2\text{Cl}_4 + \text{N}_2 \rightarrow \text{C}_2\text{Cl}_5 + \text{N}_2$ at $T = 231, 260,$ and 297 K. Solid lines are best fits of the complete data set to eq II.

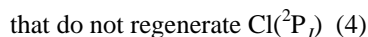
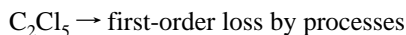
well,³⁰ although in principle F_c may vary with temperature and may be different for different reactions.^{31–33} Fitting our measured values for $k_1([\text{N}_2], T)$ to eq II gives the following parameters:

$$k_{1,0}(T) = 1.40 \times 10^{-28} (T/300)^{-8.5} \text{ cm}^6 \text{ molecule}^{-2} \text{ s}^{-1}$$

$$k_{1,\infty}(T) = 3.97 \times 10^{-11} (T/300)^{-1.2} \text{ cm}^3 \text{ molecule}^{-1} \text{ s}^{-1}$$

Experimental falloff data are compared with curves calculated using the above parameters in Figure 4. The parametrization represents the experimental data reasonably well. Variation of the parameter F_c does not significantly improve the quality of the fits.

Kinetics at $T > 330$ K. At temperatures above 330 K, chlorine atom regeneration via a secondary reaction became evident. Under these experimental conditions, observed Cl(²P_J) temporal profiles were independent of laser fluence and Cl₂ concentration but varied as a function of [C₂Cl₄], pressure, and temperature in the manner expected if unimolecular decomposition of C₂Cl₅ was the source of regenerated Cl(²P_J). Assuming that C₂Cl₅ decomposition is the source of regenerated Cl(²P_J), the relevant kinetic scheme controlling the Cl(²P_J) temporal profile includes not only reactions 1 and 3 but also reactions -1 and 4:



Assuming that all processes affecting the temporal evolution of Cl(²P_J) and C₂Cl₅ are first-order or pseudo-first-order, the rate equations for reactions 1, -1, 3, and 4 can be solved analytically:

$$S_t/S_0 = \{(Q + \lambda_1) \exp(\lambda_1 t) - (Q + \lambda_2) \exp(\lambda_2 t)\} / (\lambda_1 - \lambda_2) \quad (\text{VI})$$

where S_t and S_0 are the resonance fluorescence signal levels at times t and 0, and

$$Q = k_{-1} + k_4 \quad (\text{VII})$$

$$Q + k_3 + k_1[\text{C}_2\text{Cl}_4] = -(\lambda_1 + \lambda_2) \quad (\text{VIII})$$

$$k_3 Q + k_4 k_1[\text{C}_2\text{Cl}_4] = \lambda_1 \lambda_2 \quad (\text{IX})$$

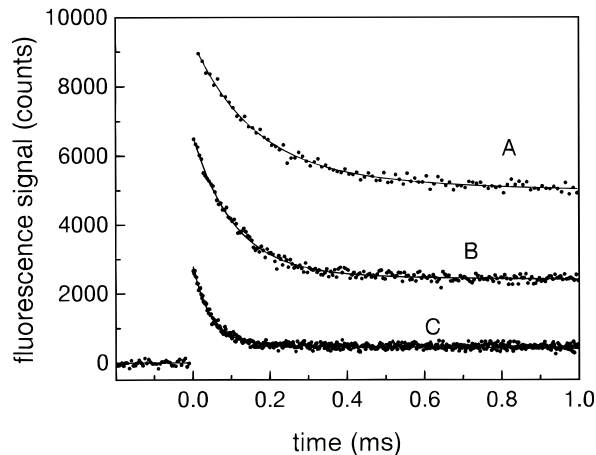


Figure 5. Typical Cl(²P_J) temporal profiles observed at $T > 330$ K. Experimental conditions: $T = 360$ K; $P = 100$ Torr; $M = \text{N}_2$; $[\text{Cl}_2] = 7.3 \times 10^{12}$ molecules cm^{-3} ; $[\text{Cl}]_0 = 1.3 \times 10^{11}$ atoms cm^{-3} ; $[\text{C}_2\text{Cl}_4]$ in units of 10^{14} molecules $\text{cm}^{-3} = (\text{A}) 1.89, (\text{B}) 3.90,$ and $(\text{C}) 11.2$; number of laser shots averaged = (A) 30 000, (B) 30 000, and (C) 40 000. Solid lines are obtained from nonlinear least-squares fits to eq VI. Best fit parameters, i.e., $\lambda_1, \lambda_2,$ and $Q,$ are summarized in Table 2. For the sake of clarity, traces B and C are scaled by factors of 1.1 and 1.5, respectively.

Observed Cl(²P_J) temporal profiles were fit to the double-exponential eq VI using a nonlinear least-squares method to obtain values for $\lambda_1, \lambda_2, Q,$ and S_0 . The background Cl(²P_J) loss rate in the absence of C₂Cl₄, i.e., k_3 , was directly measured at each temperature and pressure (see Table 2). Rearrangement of the above equations shows that the rate coefficients $k_1, k_{-1},$ and k_4 can be obtained from the fit parameters and the measured k_3 using the following equations:

$$k_1 = -(Q + k_3 + \lambda_1 + \lambda_2) / [\text{C}_2\text{Cl}_4] \quad (\text{X})$$

$$k_4 = (\lambda_1 \lambda_2 - k_3 Q) / k_1 [\text{C}_2\text{Cl}_4] \quad (\text{XI})$$

$$k_{-1} = Q - k_4 \quad (\text{XII})$$

Typical Cl(²P_J) temporal profiles observed in the high-temperature experiments are shown in Figure 5 along with best fits of each temporal profile to eq VI. The results for all high-temperature experiments are summarized in Table 2. It is worth noting that values for $k_1([\text{N}_2], T)$ obtained from analysis of the high-temperature data are consistent with those expected based on extrapolation of the results from $T < 300$ K. We believe that reported values for k_1 , even at high temperature where Cl(²P_J) regeneration is fast, are accurate to within $\pm 20\%$. Absolute uncertainties in reported values for k_{-1} are somewhat more difficult to assess. Inspection of Table 2 shows that the precision of multiple determinations of k_{-1} at a particular temperature and pressure (for varying [C₂Cl₄]) is quite good. An inherent assumption in our analysis is that the only significant C₂Cl₅ loss process that results in chlorine atom production is reaction -1; as long as this assumption is correct (it almost certainly is), we believe the absolute accuracy of our reported k_{-1} values is $\pm 30\%$ over the full range of temperature and pressure investigated.

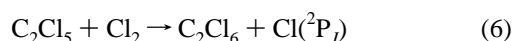
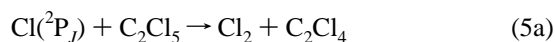
Possible Secondary Chemistry Complications. The photochemical system used to study the kinetics of reactions 1 and -1 appears to be relatively free of complications from unwanted side reactions. The only potential secondary reactions we are aware of which could destroy or regenerate chlorine atoms (other

TABLE 2: Results of the $\text{Cl}(^2\text{P}_j) + \text{C}_2\text{Cl}_4 \leftrightarrow \text{C}_2\text{Cl}_5 + \text{N}_2$ Equilibration Kinetics Experiments^a

<i>T</i>	<i>P</i>	[Cl ₂]	[Cl] _{<i>t</i>=0}	[C ₂ Cl ₄]	<i>Q</i>	−λ ₁	−λ ₂	<i>k</i> ₃	<i>k</i> ₄	<i>k</i> ₁	<i>k</i> _{−1}	<i>K</i> _p
332	25	83	1.6	1390	469	83	2130	187	57	11.2	411	60.3
		83	1.6	2650	484	86	3670	187	73	11.6	411	62.4
		83	1.6	4480	534	127	5670	187	122	11.3	412	60.7
334	100	83	1.6	6950	544	127	8910	187	124	12.0	420	62.9
		87	1.7	1190	864	96	3260	85	100	20.2	764	58.1
		87	1.7	2500	689	44	5370	85	38	18.5	651	62.7
		87	1.7	3920	869	116	8420	85	119	19.3	750	56.7
340	6.5	87	1.7	6770	1020	217	14100	85	225	19.5	795	53.9
		61	0.9	496	327	109	802	319	−63	5.34	390	29.6
		61	0.9	682	424	170	1130	444	10	6.33	414	33.0
		61	0.9	890	506	175	1240	319	93	6.61	414	34.5
		61	0.9	984	420	162	1290	444	37	5.93	383	33.4
		61	0.9	2160	467	185	1960	444	127	5.73	340	36.4
		61	0.9	3080	482	187	2410	444	141	5.42	341	34.3
340	25	61	0.9	3310	592	245	2490	319	230	5.50	362	32.8
		57	0.7	238	536	93	829	188	−188	8.32	655	27.4
		57	0.7	648	628	83	1320	188	−15	9.00	643	30.2
		57	0.7	1550	645	39	2200	188	−25	9.06	669	29.2
340	100	57	0.7	4230	757	103	5180	188	90	10.3	668	33.2
		48	0.7	452	1220	82	2050	88	74	18.2	1150	34.3
		48	0.7	955	1150	71	2860	88	60	17.7	1090	34.8
		74	1.3	1070	1270	83	3210	116	63	17.7	1200	31.7
		48	0.7	1220	1210	64	3470	88	55	17.6	1100	34.6
		48	0.7	1240	1150	66	3350	88	52	18.3	1160	34.0
		48	0.7	1340	1110	61	3440	88	49	17.2	1060	34.9
		48	0.7	1760	1120	62	4340	88	53	18.1	1070	36.7
		48	0.7	2110	1150	72	4940	88	67	17.9	1080	35.7
		74	1.3	3040	1220	73	6720	116	64	17.7	1160	32.9
350	100	57	0.9	529	2150	44	2950	61	1	14.8	2150	14.5
		210	0.7	1630	2130	17	4640	61	−21	15.1	2150	14.7
		210	3.2	1640	2300	66	4790	61	70	15.2	2230	14.3
		57	0.9	1670	2070	19	4750	61	−13	15.8	2080	15.9
		110	0.7	1670	2110	15	4780	61	−21	15.7	2130	15.5
		57	0.9	5190	2550	152	10700	61	178	15.9	2370	14.1
360	25	70	1.0	2120	2040	126	3870	148	103	8.53	1940	8.96
		70	1.0	4920	2020	98	5930	148	73	7.84	1950	8.20
		70	1.0	10700	2070	104	10500	148	94	7.88	1970	8.13
360	100	90	1.7	1110	3780	88	5460	166	−89	14.6	3870	7.71
		73	1.3	1890	3560	53	6200	92	2	13.8	3550	7.92
		73	1.3	3900	3570	43	9280	92	14	14.5	3550	8.34
		90	1.7	6290	4050	67	13200	166	23	14.5	4030	7.31
		73	1.3	11200	4120	233	21500	92	265	15.6	3860	8.25
370	25	68	1.2	4010	3230	129	6080	217	30	6.92	3200	4.29
		68	1.2	8440	3270	111	9350	217	54	7.08	3220	4.37
		68	1.2	11200	3050	50	11000	217	−15	7.01	3070	4.53
370	100	83	1.2	2910	6800	61	11100	87	20	14.7	6780	4.30
		83	1.2	5780	6240	56	13500	87	30	12.5	6210	3.99
		83	1.2	8420	6490	104	18700	87	113	14.6	6380	4.53
		83	1.2	15100	7010	319	30700	87	384	15.9	6630	4.76
380	25	73	1.0	6060	4340	99	7760	199	−28	5.48	4370	2.42
		73	1.0	12700	5110	147	13700	199	117	6.72	4990	2.60
380	100	75	1.2	2200	9820	78	11800	75	90	9.04	9730	1.79
		75	1.2	5060	9690	40	14800	75	−26	10.1	9720	2.01
		75	1.2	6280	11500	124	18700	101	158	11.5	11300	1.96
		75	1.2	9920	10700	78	21300	75	81	10.7	10600	1.95
		210	3.6	10800	9630	54	20300	75	0	9.91	9630	1.99
390	25	210	0.9	10900	10500	117	21700	75	156	10.3	10400	1.91
		89	1.0	6000	7860	174	10700	184	146	4.68	7710	1.14
		89	1.0	21400	8330	203	19000	184	218	4.97	8120	1.15
		89	1.0	24100	8260	128	20000	184	88	4.85	8170	1.12
		89	1.0	27000	8660	242	22600	184	278	5.18	8380	1.16

^a Units: *T* (K); *P* (Torr); concentrations (10¹¹ molecules cm^{−3}); *Q*, λ₁, λ₂, *k*₃, *k*₄, *k*_{−1} (s^{−1}); *k*₁ (10^{−12} cm³ molecule^{−1} s^{−1}); *K*_p (10⁴ atm^{−1}).

than reaction −1, of course) are the following:



The concentrations of photochemically generated radicals employed in this study, i.e., $\leq 3 \times 10^{11}$ cm^{−3}, were sufficiently small that a radical–radical interaction such as reaction 5 could

not be an important Cl(^2P_{*j*}) removal process even if the rate coefficient were gas kinetic. Experimentally, the fact that observed kinetics were unaffected by significant variations in [Cl]₀ confirms that reaction 5 did not contribute significantly to Cl(^2P_{*j*}) removal. The only kinetics studies of reaction 6 reported in the literature involved competitive chlorination studies where kinetic information was derived by fitting observed product distributions to a complex chemical mechanism;^{10,34} these studies, while indirect, suggest that *k*₆ is much too slow for reaction 6 to be a significant interference. Experimentally, we found that observed kinetics were unaffected

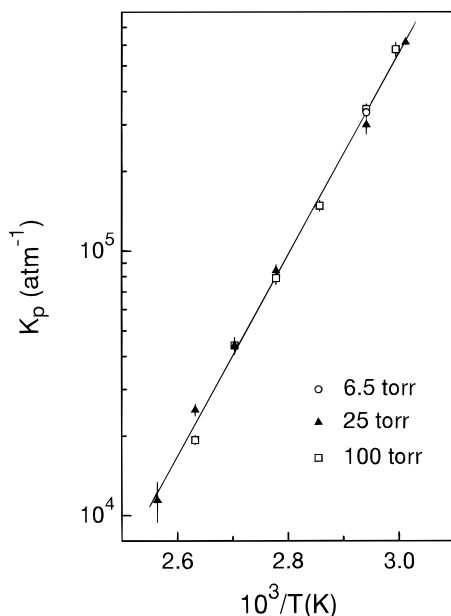


Figure 6. van't Hoff plot for the reaction $\text{Cl} + \text{C}_2\text{Cl}_4 \leftrightarrow \text{C}_2\text{Cl}_5$. The solid line is obtained from a linear least-squares analysis and gives the second-law thermochemical parameters for the reaction (see Table 4). Different symbols indicate data obtained at different total pressures.

by significant variations in Cl_2 concentration, thus confirming that reaction 6 played no role in controlling observed $\text{Cl}(\text{P}_j)$ temporal profiles.

C_2Cl_5 Thermochemistry: Second-Law Analysis. The equilibrium constants, K_p , given in Table 2 are computed from the relationship

$$K_p = k_1/k_{-1}RT = K_c/RT \quad (\text{XIII})$$

Use of eq XIII involves making the *assumption* that reaction -1 is truly the reverse of reaction 1, i.e., that the products of reaction -1 do not contain substantial internal excitation. If, for example, reaction -1 resulted in production of predominantly $\text{Cl}(\text{P}_{1/2})$, it would be inappropriate to use the ratio k_1/k_{-1} as a basis for evaluating the thermochemistry of reaction 1. While it seems reasonable to assume that energy is distributed statistically in the translational and internal degrees of freedom of the C_2Cl_4 and $\text{Cl}(\text{P}_j)$ products of reaction -1, it should be kept in mind that there presently exists no experimental verification that this assumption is correct.

Assuming that K_p can be computed from the ratio of measured values for k_1 and k_{-1} , a van't Hoff plot, i.e., a plot of $\ln K_p$ versus T^{-1} , can be constructed; such a plot is shown in Figure 6. Since

$$\ln K_p = (\Delta S/R) - (\Delta H/RT) \quad (\text{XIV})$$

the enthalpy change associated with reaction 1 is obtained from the slope of the van't Hoff plot while the entropy change is obtained from the intercept. At 360 K, the midpoint of the experimental T^{-1} range, this "second-law analysis" gives the results $\Delta H = -17.5 \pm 0.6 \text{ kcal mol}^{-1}$ and $\Delta S = -26.1 \pm 1.8 \text{ cal mol}^{-1} \text{ K}^{-1}$, where the errors are 2σ and represent precision only.

C_2Cl_5 Thermochemistry: Third-Law Analysis. In addition to the second-law analysis described above, we have also carried out a third-law analysis, where the experimental value of K_p at 360 K ($79\,800 \pm 8000 \text{ atm}^{-1}$) has been employed in conjunction with a calculated entropy change to determine ΔH .

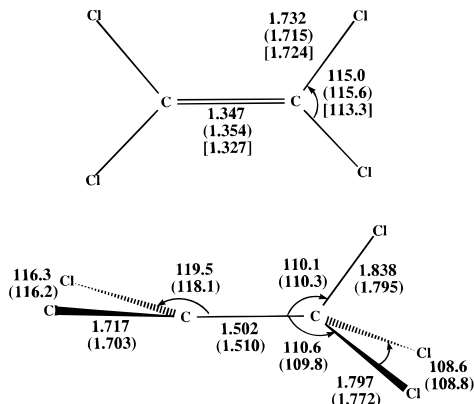


Figure 7. Structure for C_2Cl_4 and C_2Cl_5 derived from *ab initio* calculations at the Becke3LYP/6-31+G(d) level as discussed in the text. Bond lengths and bond angles shown in parentheses are at the MP2/6-31+G(d) level of theory and values for C_2Cl_4 in square brackets are recommendations from the JANAF tables (ref 46).

Since experimental data concerning the structure of C_2Cl_5 are not available, *ab initio* calculations have been carried out for this species. The calculations employed density functional theory³⁵⁻³⁷ as implemented in the GAUSSIAN 92/DFT program system.³⁸ With an appropriate choice of gradient correction and a modest basis set, DFT has been shown to frequently give results of near chemical quality.³⁹⁻⁴⁴ In addition, spin contamination does not seem to be as serious for DFT compared to Hartree-Fock (HF) theory.⁴⁵ Becke3LYP, which seems to be a good choice of exchange and correlational functional, has been used with the 6-31+G(d) basis set to optimize geometries for C_2Cl_5 . Vibrational frequencies have been calculated with the same method. The results for C_2Cl_4 can be compared with experiment to lend credibility to the approach while the results for C_2Cl_5 can be employed to compute its absolute entropy as well as heat capacity corrections. As a check on the DFT results, MP2/6-31+G(d) optimizations were also carried out for C_2Cl_4 and C_2Cl_5 . Only small differences in the geometries were noted. Since the DFT results were closer to experiment for C_2Cl_4 , the DFT geometries and frequencies for C_2Cl_5 were used in the third-law analysis.

Two distinctly different $\text{Cl}(\text{P}_j)\text{-C}_2\text{Cl}_4$ adducts are possible. A chlorine atom could add symmetrically to $\text{Cl}_2\text{C}=\text{CCl}_2$ to form a π -complex or a three-membered ring with unpaired spin density on chlorine. Alternatively, a chlorine atom could add unsymmetrically to form a σ -complex with unpaired spin density on the β -carbon. Our calculations predict that the most stable form for C_2Cl_5 is the haloalkyl radical CCl_3CCl_2 , i.e., the σ -complex. Calculated structures for C_2Cl_4 and C_2Cl_5 are shown in Figure 7. For comparison, experimental bond lengths and bond angle for C_2Cl_4 ⁴⁶ are also shown in Figure 7; the calculated structure of C_2Cl_4 is in good agreement with experiment.

To carry out the third-law analysis, absolute entropies as a function of temperature were obtained from the JANAF tables⁴⁶ for $\text{Cl}(\text{P}_j)$, calculated using vibrational frequencies and moments of inertia taken from the JANAF tables for C_2Cl_4 ,⁴⁷ and calculated using the moments of inertia and vibrational frequencies in Table 3 for C_2Cl_5 . The moments of inertia in Table 3 were computed using the C_2Cl_5 structure shown in Figure 7. The vibrational frequencies in Table 3 were calculated using the approach described above. Because calculated vibrational frequencies for C_2Cl_4 are very close to those given in the JANAF tables,⁴⁶ no scaling of the C_2Cl_5 frequencies is deemed necessary. At 360 K, the third-law analysis gives the results $\Delta H = -18.6 \pm 0.5 \text{ kcal mol}^{-1}$ and $\Delta S = -29.3 \pm 1.0 \text{ cal mol}^{-1} \text{ K}^{-1}$;

TABLE 3: Summary of Parameters Used in Calculations of Absolute Entropies and Heat Capacity Corrections

species	ν (cm ⁻¹)	σ	I_{ABC} (amu ³ Å ⁶)	g_0	g_1	$\Delta\epsilon$ (cm ⁻¹) ^a
Cl				4	2	882.36
C ₂ Cl ₄	1571 1000 918 777 512 447 347 324 288 235 176 110	4	7.50 × 10 ⁷	1		
C ₂ Cl ₅	1124 942 782 721 624 447 406 342 327 264 233 231 173 129 39	6	1.76 × 10 ⁸	2		

^a $\Delta\epsilon \equiv$ assumed energy splitting between lowest two electronic states. C₂Cl₄ has no low-lying excited electronic states, and C₂Cl₅ is assumed to have none.

TABLE 4: Thermochemical Parameters for the Reaction Cl(²P_J) + C₂Cl₄ → C₂Cl₅^a

T	method	$-\Delta H$	$-\Delta S$	$\Delta H_{f,T}^{\circ}(\text{C}_2\text{Cl}_5)^b$
360	2nd law	17.5 ± 0.6	26.1 ± 1.8	
	3rd law	18.6 ± 0.5	29.3 ± 1.0	
298	2nd law	17.5 ± 0.7	26.2 ± 1.9	8.5 ± 0.8
	3rd law	18.7 ± 0.6	29.4 ± 1.0	7.4 ± 0.7
0	2nd law	17.1 ± 0.8		8.7 ± 0.9
	3rd law	18.2 ± 0.7		7.5 ± 0.8

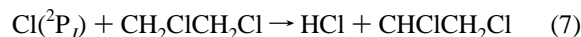
^a Units: T (K); ΔH , $\Delta H_{f,T}^{\circ}(\text{C}_2\text{Cl}_5)$ (kcal mol⁻¹); ΔS (cal mol⁻¹ K⁻¹).
^b Calculated using values for $\Delta H_{f,T}^{\circ}(\text{Cl})$ and $\Delta H_{f,T}^{\circ}(\text{C}_2\text{Cl}_4)$ taken from ref 46.

the uncertainties we report reflect an estimate of the uncertainties introduced by our imperfect knowledge of the input data needed to calculate absolute entropies (the low frequency vibrations of C₂Cl₅ are most significant) as well as our estimated uncertainty in the experimental value for $K_p(360\text{ K})$.

Summary of Thermochemical Results. The thermochemical results of this study are summarized in Table 4. Appropriate heat capacity corrections have been employed to obtain ΔH values at 298 and 0 K. Using literature values⁴⁶ for the heats of formation of Cl(²P_J) and C₂Cl₄ at 298 and 0 K allows the heat of formation of C₂Cl₅ to be evaluated. As can be seen from Table 4, the agreement between the second- and third-law results is not perfect. Since the uncertainties in the $\Delta H_{f,T}^{\circ}(\text{C}_2\text{Cl}_5)$ values obtained by the two methods are about the same, it seems appropriate to report simple averages of the second- and third-law values, while adjusting reported uncertainties to encompass the 2 σ error limits of both determinations. Using this approach, we report $\Delta H_{f,298}^{\circ}(\text{C}_2\text{Cl}_5) = 8.0 \pm 1.3$ kcal mol⁻¹ and $\Delta H_{f,0}^{\circ}(\text{C}_2\text{Cl}_5) = 8.1 \pm 1.5$ kcal mol⁻¹. The Cl–C bond energy can also be directly calculated from theory, where single-point energies are determined with an expanded basis set and zero-point corrections are made with DFT frequencies. The predicted bond energy at 0 K is 14.2 kcal mol⁻¹ at Becke3LYP/

6-311+G(3df) (using the DFT geometry) and 20.3 kcal mol⁻¹ at PMP2/6-311+G(3df) (using the MP2 geometry). While the spin-projected PMP2 value is in reasonable agreement with experiment, the DFT value is several kcal mol⁻¹ too small. It appears that the DFT method calculates the relative strength of the C–C π bond to be too strong relative to the Cl–C σ bond. In a very recent assessment of computational methods for calculating radical addition reactions to alkenes, Wong and Radom found that addition enthalpies may be too positive by DFT by as much as 10 kcal mol⁻¹ when compared to QCISD results.⁴⁸ In light of their work, the underestimation of the Cl–C bond energy by DFT is not unexpected.

Comparison with Previous Research. Although this study represents the first systematic investigation of the temperature and pressure dependence of k_1 , there are several published measurements with which our results can be compared. Davis et al.,¹⁴ in one of the pioneering applications of the flash photolysis–resonance fluorescence technique, measured k_1 at 298 K in helium buffer gas; they reported rate coefficients of 4.8×10^{-12} and 6.10×10^{-12} cm³ molecule⁻¹ s⁻¹ at pressures of 15 and 100 Torr, respectively. The magnitude of Davis et al.'s rate coefficients seems a little low compared to values one might expect based on our measurements in N₂ buffer gas, and the ratio $k_1(100\text{ Torr of He})/k_1(15\text{ Torr of He}) = 1.25$ obtained from Davis et al.'s results is smaller than one would predict based on the 297 K falloff curve we have obtained using N₂ as the buffer gas (Figure 4). Breitbarth and Rottmayer have employed a discharge flow system with an EPR detector to study the kinetics of the O(³P_J) + C₂Cl₄ reaction at 298 K and 0.3 Torr total pressure in O₂ buffer gas.¹⁵ They observed that Cl(²P_J) was produced as a reaction product and, by following the temporal evolution of both O(³P_J) and Cl(²P_J), extracted a value of 3×10^{-13} cm³ molecule⁻¹ s⁻¹ for k_1 ; this value is slower than one would predict from extrapolation of our 297 K falloff curve down to $P = 0.3$ Torr under the assumption that N₂ and O₂ are equally efficient as third body colliders. In addition to the two “direct” studies discussed above, there have been a number of competitive kinetics studies of reaction 1,^{9–13,16} two of which^{13,16} report results where meaningful comparisons can be made with our results. Franklin et al. employed CW photolysis of Cl₂ in conjunction with gas chromatographic detection of C₂Cl₄; they employed the reference reactants C₂H₆ and CH₂ClCH₂Cl to measure the ratios $k_7/k_1 = 0.0295$ at 310 K and $k_8/k_1 = 1.66$ at 348 K.



Assuming $k_7(310\text{ K}) = 1.7 \times 10^{-12}$ cm³ molecule⁻¹ s⁻¹⁴⁹ and $k_8(348\text{ K}) = 5.9 \times 10^{-11}$ cm³ molecule⁻¹ s⁻¹,³⁰ Franklin et al.'s data give $k_1(310\text{ K}) = 5.8 \times 10^{-11}$ cm³ molecule⁻¹ s⁻¹ and $k_1(348\text{ K}) = 3.6 \times 10^{-11}$ cm³ molecule⁻¹ s⁻¹; these rate coefficients are not quantitatively consistent with each other but are in approximate agreement with the values expected based on our data, given the more efficient third-body colliders employed in the Franklin et al. study.⁵⁰ Atkinson and Aschmann have also employed CW photolysis of Cl₂ in conjunction with gas chromatographic detection of C₂Cl₄ and ethylene to measure $k_9/k_1 = 2.56$ at 298 K in 735 Torr of air.



Assuming $k_9(298\text{ K}, 735\text{ Torr of air}) = 1.040 \times 10^{-10}$ cm³ molecule⁻¹ s⁻¹,³⁰ the Atkinson and Aschmann¹⁶ data give $k_1(298\text{ K}, 735\text{ Torr of air}) = 4.1 \times 10^{-11}$ cm³ molecule⁻¹ s⁻¹;

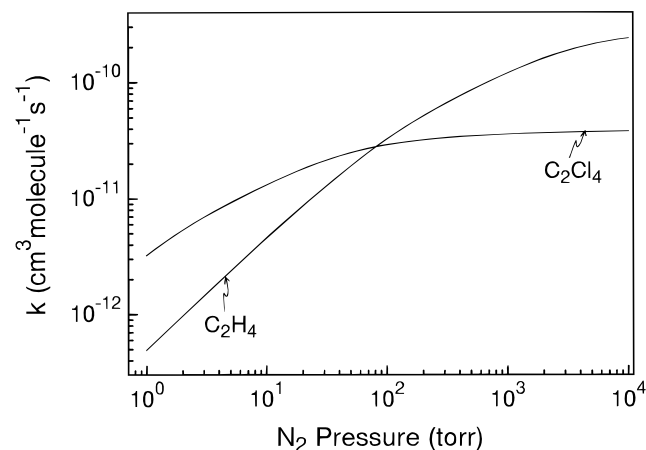


Figure 8. Falloff curves (298 K) for reactions of $\text{Cl}(^2\text{P}_j)$ with C_2Cl_4 and C_2H_4 . The C_2Cl_4 curve is calculated from falloff parameters determined in this study while the C_2H_4 curve is calculated from the falloff parameters recommended in ref 30.

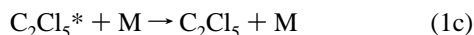
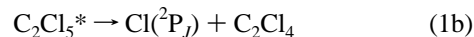
this is slightly faster than the value we report but in agreement within combined experimental uncertainties.

Franklin et al.¹³ in their competitive kinetics studies (described above) derived the following relationship from their data: $\log(k_{-1}/k_1k_6) = 4.90 - 10650/4.576T \text{ mol}^2 \text{ L}^{-2} \text{ s}$. They used their determinations of k_1 in conjunction with the measurements of $k_6(T)$ reported by Dusdeil et al.³⁴ to obtain values for $k_{-1}(T)$. Franklin et al.'s values, when corrected for updated information about $k_7(T)$ and $k_8(T)$, give values for $k_{-1}(T)$ which are somewhat faster than the values we report. A more quantitative comparison does not appear to be worthwhile because (a) the Arrhenius expression for $k_6(T)$ is highly uncertain,^{10,34} (b) Franklin et al. report k_{-1} to be pressure independent while we find k_{-1} to be pressure dependent (Table 2), and (c) as mentioned above, Franklin et al. employed more efficient third-body colliders (C_2Cl_4 , Cl_2 , C_2H_6 , $\text{CH}_2\text{ClCH}_2\text{Cl}$, CO_2 , and SF_6) in their study than we did in ours (N_2). From their evaluations of k_1 and k_{-1} at two temperatures, Franklin et al. derived $\Delta H = -16.9 \pm 1.0 \text{ kcal mol}^{-1}$, i.e., somewhat higher than the value we report but in agreement within combined experimental uncertainties. (We believe the uncertainty in the Franklin et al. determination of ΔH is actually considerably larger than their published estimate¹³ of $\pm 1.0 \text{ kcal mol}^{-1}$.)

The best fit value for the parameter n (describing the temperature dependence of $k_{1,0}$) obtained in this study, i.e., $n = 8.5$, is larger than is typically found for association reactions of atmospheric interest.³⁰ Recommended values of n for 62 atmospheric association reactions range from 0.0 to 6.7, with the largest values found for the $\text{CF}_2\text{ClO}_2 + \text{NO}_2$ and $\text{CCl}_3 + \text{O}_2$ reactions.³⁰ Interestingly, both $\text{CF}_2\text{ClO}_2\text{NO}_2$ and CCl_3O_2 are relatively weakly bound species, with bond strengths only a few kcal mol^{-1} stronger^{51,52} than that of C_2Cl_5 . While the results reported in this paper clearly demonstrate that k_1 increases significantly with decreasing temperature, the value of n is rather uncertain because no data were obtained at pressures anywhere near the low-pressure limit. As a result, extrapolation of our results outside of the experimental temperature regime should be carried out with caution.

The 298 K falloff curves for $\text{Cl}(^2\text{P}_j)$ reactions with C_2H_4 and C_2Cl_4 over the pressure range 1–10 000 Torr of N_2 are compared in Figure 8. The C_2Cl_4 curve is based on the falloff parameters determined in this study while the C_2H_4 curve is calculated from the falloff parameters recommended by the NASA panel for chemical kinetics and photochemical data evaluation,³⁰ which are based on the experimental data of Wallington et al.⁵³ over the pressure range 10–3000 Torr.

Interestingly, $\text{Cl}(^2\text{P}_j)$ reacts much more rapidly with C_2Cl_4 than with C_2H_4 in the low-pressure limit, but much more rapidly with C_2H_4 than with C_2Cl_4 in the high-pressure limit. This interesting reactivity pattern can be rationalized in terms of the simple Lindemann–Hinshelwood mechanism,^{54,55} where reaction 1, for example, proceeds via the following three-step process:



If one makes the steady state approximation for the energized adduct, C_2Cl_5^* , the low- and high-pressure limit rate coefficients are obtained as $k_{1,0} = k_{1a}k_{1c}/k_{1b}$ and $k_{1,\infty} = k_{1a}$. The fact that $k_{9,\infty} > k_{1,\infty}$ implies that $\text{Cl}(^2\text{P}_j)$ adds more rapidly to C_2H_4 than to C_2Cl_4 to form the energized species $\text{C}_2\text{H}_5\text{-}n\text{Cl}_n^*$; this seems reasonable since the four chlorine atoms in C_2Cl_4 would be expected to sterically hinder approach of $\text{Cl}(^2\text{P}_j)$ to a carbon atom. The fact that $k_{9,0} < k_{1,0}$ also seems reasonable since collisional deactivation of $\text{C}_2\text{H}_5\text{-}n\text{Cl}_n^*$ would be expected to be more efficient for C_2Cl_5^* than for $\text{C}_2\text{H}_4\text{Cl}^*$ due to the much higher density of states in C_2Cl_5^* .

Implications for Atmospheric Chemistry. The results reported in this paper confirm that C_2Cl_4 reacts with $\text{Cl}(^2\text{P}_j)$ several hundred times faster than with OH under atmospheric conditions. Hence, in selected atmospheric environments such as the marine boundary layer, where $\text{Cl}(^2\text{P}_j)$ levels appear to be particularly high,^{17–19} reaction with $\text{Cl}(^2\text{P}_j)$ will be the dominant atmospheric removal mechanism for C_2Cl_4 . In addition, C_2Cl_4 is being employed as a “tracer” for analyzing the potential importance of chlorine atoms as an oxidant in the free troposphere;⁵⁶ the temperature- and pressure-dependent values for $k_1(T,P)$ reported in this study are useful for making such an analysis as quantitative as possible.

Acknowledgment. The experimental component of this research was supported by the National Aeronautics and Space Administration, Upper Atmosphere Research Program, through Grant NAGW-1001 to Georgia Institute of Technology. Computer time for this study was made available by the Alabama Supercomputer Network and the NSF-supported Pittsburgh Supercomputer Center. We thank C. A. Piety for helping with some of the experiments.

References and Notes

- Wiedmann, T. O.; Guthner, B.; Class, T. J.; Ballschmiter, K. *Environ. Sci. Technol.* **1994**, *28*, 2321.
- Franklin, J. *Toxicol. Environ. Chem.* **1994**, *46*, 169.
- Wang, C. J.-L.; Blake, D. R.; Rowland, F. S. *Geophys. Res. Lett.* **1995**, *22*, 1097.
- Singh, H. B. In *Composition, Chemistry, and Climate of the Atmosphere*; Singh, H. B., Ed.; Van Nostrand Reinhold: New York, 1995; pp 216–250.
- Winer, A. M.; Lloyd, A. C.; Darnall, K. R.; Pitts, J. N., Jr. *J. Phys. Chem.* **1976**, *80*, 1635.
- Howard, C. J. *J. Chem. Phys.* **1976**, *65*, 4771.
- Chang, J. S.; Kaufman, F. *J. Chem. Phys.* **1977**, *66*, 4989.
- Kirchner, J.; Helf, D.; Ott, P.; Vogt, S. *Ber. Bunsen-Ges. Phys. Chem.* **1990**, *94*, 77.
- Goldfinger, P.; Jeunehomme, M.; Martens, G. *J. Chem. Phys.* **1958**, *28*, 456.
- Ayscough, P. B.; Cocker, A. J.; Dainton, F. S.; Hirst, S.; Weston, M. *Proc. Chem. Soc., London* **1961**, 244.
- Goldfinger, P.; Huybrechts, G.; Martens, G. *Trans. Faraday Soc.* **1961**, *57*, 2210.
- Knox, J.; Waugh, K. C. *Trans. Faraday Soc.* **1969**, *65*, 1585.

- (13) Franklin, J. A.; Huybrechts, G.; Cillien, C. *Trans. Faraday Soc.* **1969**, *65*, 2094.
- (14) Davis, D. D.; Braun, W.; Bass, A. M. *Int. J. Chem. Kinet.* **1970**, *2*, 101.
- (15) Breitbarth, F.-W.; Rottmayer, S. *Plasma Chem. Plasma Proc.* **1986**, *6*, 381.
- (16) Atkinson, R.; Aschmann, S. M. *Int. J. Chem. Kinet.* **1987**, *19*, 1097.
- (17) Jobson, B. T.; Niki, H.; Yokouchi, Y.; Bottenheim, J.; Hopper, F.; Leaich, R. *J. Geophys. Res.* **1994**, *99*, 25355.
- (18) Singh, H. B.; Gregory, G. L.; Anderson, B.; Browell, E.; Sachse, G. W.; Davis, D. D.; Crawford, J.; Bradshaw, J. D.; Talbot, R.; Blake, D. R.; Thornton, D.; Newell, R.; Merrill, J. *J. Geophys. Res.*, in press.
- (19) Finlayson-Pitts, B. J. *Res. Chem. Intermed.* **1993**, *19*, 235.
- (20) Singh, H. B.; Lillian, D.; Appleby, A.; Lobban, L. *Environ. Lett.* **1975**, *10*, 253.
- (21) Stickel, R. E.; Nicovich, J. M.; Wang, S.; Zhao, Z.; Wine, P. H. *J. Phys. Chem.* **1992**, *96*, 9875 and references therein.
- (22) Nicovich, J. M.; Wang, S.; Wine, P. H. *Int. J. Chem. Kinet.* **1995**, *27*, 359.
- (23) Stated minimum purity of liquid phase in high-pressure cylinder.
- (24) Busch, G. E.; Mahoney, R. T.; Morse, R. I.; Wilson, K. R. *J. Chem. Phys.* **1969**, *51*, 449.
- (25) Park, J.; Lee, Y.; Flynn, G. W. *Chem. Phys. Lett.* **1991**, *186*, 441.
- (26) Tyndall, G. S.; Orlando, J. J.; Kegley-Owen, C. S. *J. Chem. Soc., Faraday Trans.* **1995**, *91*, 3055.
- (27) Fletcher, I. S.; Husain, D. *Chem. Phys. Lett.* **1977**, *49*, 516.
- (28) Clark, R. H.; Husain, D. *J. Photochem.* **1983**, *21*, 93.
- (29) Chichinin, A. I.; Krasnoperov, L. N. *Chem. Phys. Lett.* **1989**, *160*, 448.
- (30) DeMore, W. B.; Sander, S. P.; Golden, D. M.; Hampson, R. F.; Kurylo, M. J.; Howard, C. J.; Ravishankara, A. R.; Kolb, C. E.; Molina, M. J. *Chemical Kinetics and Photochemical Data for Use in Stratospheric Modeling*; Evaluation No. 11, Jet Propulsion Laboratory Publication 94-26, 1994.
- (31) Troe, J. *J. Phys. Chem.* **1979**, *83*, 114.
- (32) Luther, K.; Troe, J. *Proc. 17th Int. Symp. Combust.* **1978**, 535.
- (33) Troe, J. *Ber. Bunsen-Ges. Phys. Chem.* **1983**, *87*, 161.
- (34) Dusdeil, S.; Goldfinger, P.; Mahieu-Van Der Auwera, A. M.; Martens, G.; Van Der Auwera, D. *Trans. Faraday Soc.* **1961**, *57*, 2197.
- (35) Parr, R. G.; Yang, W. *Density-Functional Theory of Atoms and Molecules*; Oxford Press: Oxford, United Kingdom, 1989.
- (36) Ziegler, T. *Chem. Rev.* **1991**, *91*, 651.
- (37) *Density Functional Methods in Chemistry*; Labanowski, J., Andzelm, J. W., Eds.; Springer-Verlag: Berlin, 1991.
- (38) Frisch, M. J.; Trucks, G. W.; Schlegel, H. B.; Gill, P. M. W.; Johnson, B. G.; Wong, M. W.; Foresman, J. B.; Robb, M. A.; Head-Gordon, M.; Replogle, E. S.; Gomperts, R.; Andres, J. L.; Raghavachari, K.; Binkley, J. S.; Gonzales, C.; Martin, R. L.; Fox, D. J.; DeFrees, D. J.; Baker, J.; Stewart, J. J. P.; Pople, J. A. *Gaussian 92/DFT (Rev. G. 2)*; Gaussian, Inc.: Pittsburgh, PA, 1993.
- (39) Johnson, B. G.; Gill, P. M. W.; Pople, J. A. *J. Chem. Phys.* **1993**, *98*, 5612.
- (40) Becke, A. D. *J. Chem. Phys.* **1993**, *98*, 5648.
- (41) Gill, P. M. W.; Johnson, B. G.; Pople, J. A.; Frisch, M. J. *Chem. Phys. Lett.* **1992**, *197*, 499.
- (42) Raghavachari, K.; Strout, D. L.; Odom, G. K.; Scuseria, G. E.; Pople, J. A.; Johnson, B. G.; Gill, P. M. W. *Chem. Phys. Lett.* **1993**, *214*, 357.
- (43) Raghavachari, K.; Zhang, B.; Pople, J. A.; Johnson, B. G.; Gonzales, C. A.; Gill, P. M. W.; Pople, J. A. *Chem. Phys. Lett.* **1994**, *220*, 385.
- (44) Johnson, B. G.; Gonzales, C. A.; Gill, P. M. W.; Pople, J. A. *Chem. Phys. Lett.* **1994**, *221*, 100.
- (45) Baker, J.; Scheiner, A.; Andzelm, J. *Chem. Phys. Lett.* **1993**, *216*, 380.
- (46) Chase, M. W., Jr.; Davies, C. A.; Downey, J. R., Jr.; Frurip, D. J.; McDonald, R. A.; Syverud, A. N. *J. Phys. Chem. Ref. Data* **1985**, *14* (Suppl. I).
- (47) We believe that the C₂Cl₄ absolute entropies as a function of temperature tabulated in ref 46 are incorrect.
- (48) (a) Wong, M. W.; Radom, L. *J. Phys. Chem.* **1995**, *99*, 8582. (b) For example, the reaction enthalpy for addition of *tert*-butyl radical to C₂H₄ is too positive by DFT by 9.8 kcal/mol compared to QCISD.
- (49) Wine, P. H.; Semmes, D. H. *J. Phys. Chem.* **1983**, *87*, 3572.
- (50) In their 310 K experiments, Franklin et al. (ref 13) employed gas mixtures containing 80 Torr of Cl₂, 5–20 Torr of C₂Cl₄, 25–100 Torr of CH₂ClCH₂Cl, and 0–500 Torr of CO₂ or SF₆. In their 348 K experiments, the gas mixtures contained 100 Torr of C₂Cl₄, 20 Torr of C₂H₆, and 50–400 Torr of Cl₂. No systematic dependence of *k*₁ on total pressure was reported.
- (51) Xiong, J. Q.; Carr, R. W. *J. Phys. Chem.* **1994**, *98*, 9811.
- (52) Russell, J. J.; Seetula, J. A.; Gutman, D.; Danis, F.; Caralp, F.; Lightfoot, P. D.; Lesclaux, R.; Melius, C. F.; Senkan, S. M. *J. Phys. Chem.* **1990**, *94*, 3277.
- (53) Wallington, T. J.; Andino, J. M.; Lorkovic, I. M.; Kaiser, E. W.; Marston, G. *J. Phys. Chem.* **1990**, *94*, 3644.
- (54) Lindemann, F. A. *Trans. Faraday Soc.* **1922**, *17*, 598.
- (55) Hinshelwood, C. N. *The Kinetics of Chemical Change*; Oxford University Press: Oxford, 1940.
- (56) Singh, H. B. Private communication.